Development of Probabilistic Stress Life Curves and Probabilistic Miner's Damage Distribution Using Fatigue

J.D. Ocampo* **and H.R. Millwater†**
University of Texas at San Antonio, San Antonio, Texas, 78249

Miner's rule dictates that failure occurs when the damage index (*D*) exceeds one. However, numerous comparisons with test results show that failure occurs for a range of damage index values and the results are case and material dependent. In this research, probabilistic stress-life (P-S-N) curves and the probability distribution of *D* were developed for aluminum 2024-T3 coupons as a function of stress severity factors and spectrum type through simulations of variable amplitude tests. Ten simulations of variable amplitude tests for a Normal spectrum and six for an Acrobatic spectrum were carried out for general aviation aircraft. Probabilistic S-N curves were constructed from constant amplitude tests and queried during the simulation of the variable amplitude tests. The results for *D* were best represented by a Weibull distribution with the mean values ranging from approximately 0.72 for low severity Normal usage open hole coupon to 5.73 for high severity normal usage 50% load transfer coupon, and from 0.74 for low severity Acrobatic open hole coupon to 4.39 for high severity acrobatic usage 50% load transfer. The probabilistic results for *D* can be used within a probabilistic simulation of fatigue failure of a general aviation structure.

I. Introduction and Overview

DURING the last sixty years, the Palmgren-Miner linear cumulative damage rule has been the most common method used for determining life for variable amplitude fatigue because of its simplicity[1]. Although Palmgren-Miner's rule is easy to implement, it has a potential drawback of non-agreement with experimental results. The reasons for the drawback are: i) cycles with a stress amplitude below the fatigue limit are assumed to be not damaging, whereas, in reality, their effect is compounded with the damage associated with cycles of amplitudes above the fatigue limit, ii) sequence effects of loading are ignored, iii) localized notch root plasticity leads to residual stresses which can affect the fatigue damage of subsequent cycles and others[2].

Several tests in the literature found that the Palmgren-Miner Rule did not always give reliable predictions when the failure constant is fixed to one; failure occurs sometimes for values below and above one[3].

In this research, Probabilistic Stress-life (P-S-N) curves were developed from constant amplitude tests[4] and a probability distribution of the failure damage index was developed for aluminum 2024-T3 coupons as a function of Stress Severity Factors (SSF)[5] and spectrum type through simulations of variable test results.

* Graduate Research Assistant, Mechanical Engineering, One UTSA Circle, and AIAA Member.
† Associate Professor, Mechanical Engineering, One UTSA Circle, and AIAA Member.

II. Methodology

This section describes the methodology used to develop the P-S-N curves and the Stress Severity Factor (SSF), and finally the failure Damage Index (D). First, a standard practice[6] to fit the constant amplitude S-N testing results is presented, then the SSF parameters are developed based on the P-S-N curves, and finally the failure Damage Index is constructed and presented.

A. Probabilistic Stress-Life and Stress Severity Factor

To construct the P-S-N curves, constant amplitude fatigue test results developed under an experiments conducted in a research program by Wichita State University[4] were used. The test data were developed for different coupon configurations at different maximum stress levels and mean stress. A summary of the data available for this study is shown in Table 1.

Coupon Configuration	Maximum Stress [KSI]	Number of Data Points	Mean Stress [KSI]
Open Hole	42, 32, 18, 12, 10, and 9.25	41	3
Open Hole	42, 32, 20, 18, 12.5, and 11.5	46	6
Hilok Filled Hole	42, 32, 24, 18, and 14	32	3
Hilok Filled Hole	42, 32, 30, 24, 21 and 16	37	6
Hilok 30 % Load Transfer	42, 32, 24, 15, and 8	38	3
Hilok 30 % Load Transfer	42, 32, 24, 15, and 11	36	6
Hilok 50 % Load Transfer	42, 32, 24, 15, and 8	37	3
Hilok 50 % Load Transfer	42, 32, 24, 15, and 11	45	6

Table 1. Data Available to Develop P-S-N Curves

The P-S-N curves were constructed by fitting the test data employing "The Standard Practice for Statistical Analysis of Linear or Linearized Stress-Life (S-N) and Strain-Life (ε-N) Fatigue Data" (ASTM E739)[6]. The method described by the standard assumes that the data is linear in logarithmic space. Run-outs or suspended tests are not included in the fitting. The following equation describes the method:

$$\log N = A + B(\log S) \tag{1}$$

where N is the life at the maximum value of constant amplitude cyclic stress S.

The maximum likelihood estimators of A and B can be calculated using the following equations:

$$\hat{B} = \frac{\sum_{i=1}^{k}(X_i - \overline{X})(Y_i - \overline{Y})}{\sum_{i=1}^{k}(X_i - \overline{X})^2} \tag{2}$$

$$\hat{A} = \overline{Y} + \hat{B}\overline{X} \tag{3}$$

where X represents $\log S$ and Y represents $LogN$ and k denotes the number of data points.

Some P-S-N fitting results using the ASTM method are presented in the results section.

Realizations of the P-S-N curves were randomly generated using an F-distribution and Bernoulli distribution with the following equation (the Bernoulli distribution is used to randomly sample the ± sign).

$$\hat{Y}_r = \hat{A} + \hat{B} \pm \sqrt{2F_p}\hat{\sigma}\left[\frac{1}{k} + \frac{\left(X - \bar{X}\right)^2}{\sum_{i=1}^{k}\left(X_i - \bar{X}\right)^2}\right]^{\frac{1}{2}} \tag{4}$$

Where F_p denotes the F distribution, k represents the number of data points, and the variance is described by

$$\hat{\sigma}^2 = \frac{\sum_{i=1}^{k}\left(Y_i - \hat{Y}_i\right)^2}{k-2} \tag{5}$$

Once the P-S-N curves have been developed, realizations of the different curves can be made and the SSF parameter can be developed.

The SSF is a fatigue quality number that emphasizes the fatigue characteristics of the structure rather than its static strength.

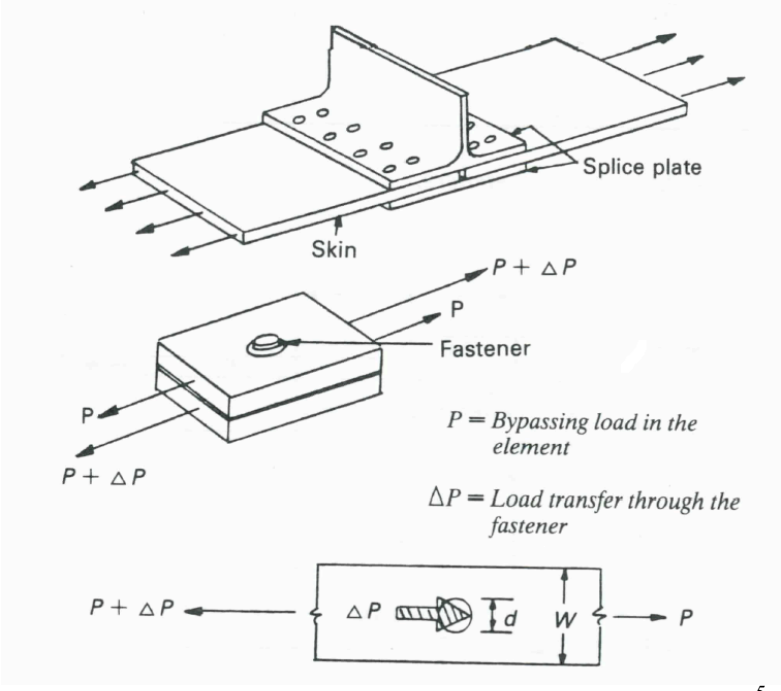

Figure 1. Load Fastener, Load Transfer, and Bypass Load[5]

The SSF is defined by the following equation.

$$SSF = \frac{\alpha \cdot \beta}{S}\left(K_{tb} \times \theta \times \frac{\Delta P}{d \cdot t} + K_{tg} \times \frac{P}{w \cdot t}\right) \tag{6}$$

Where K_{tg} is the stress concentration factor for the gross area, K_{tb} is the stress concentration factor for the bearing stress, P is the bypassing load, ΔP is the load transfer through the fastener, α accounts for the hole quality, β is the hole filling factor that accounts for the interference between the fastener and the hole, θ is the bearing distribution factor that accounts for the effect of non-uniformity of bearing stress on the hole surface, w is the width of the specimen, t is the thickness of the specimen, and d is the diameter of the fastener, see Figure 1.

The different parameters of the SSF can be developed for different specimens where the amount of transferred load and bypass load is known. The hole quality value α is 1.0 for standard holes and 0.9 for drilled and reamed holes. The SSF can be written as a function of the unknown parameters, β and θ, by identifying the ratios of fatigue strength of different specimens with the inverse ratios of their SSF numbers[5].

The β parameter is developed using the tested open hole (OH) data and the tested filled hole (FH) data. In order to generate the parameter, it is necessary to identify the ratios of fatigue strength with the inverse ratios of their SSF numbers as shown in Equation 7 and in Figure 2.

$$\frac{S(N_f)_{OH}}{S(N_f)_{FH}} = \frac{SSF_{FH}}{SSF_{OH}} \tag{7}$$

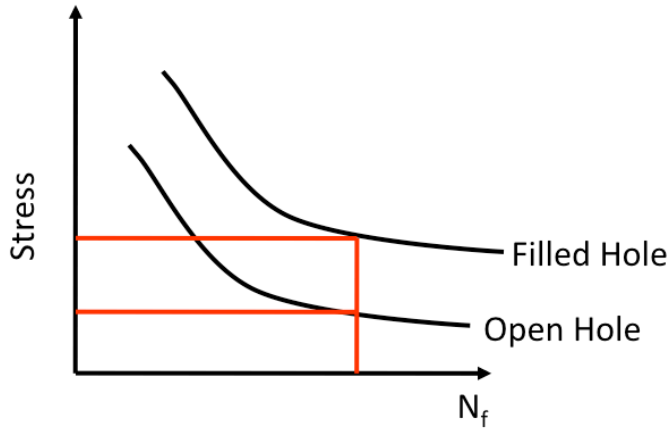

Figure 2. Hilok 30% Load Transfer 3 KSI Mean Stress

To generate β as a function of life, it is necessary to sweep through the life values and read the stress values $S(N_f)$ for the OH and FH configurations at that specific life. Then, assuming by definition $\beta_{OH} = 1$, $\alpha_{OH} = 1$, $\alpha_{FH} = 1$, and knowing that for FH and OH the load transfer is zero, β_{FH} can be computed from Equation 8. K_{tg} values cancel out because the geometry of both coupons is the same.

$$\frac{S(N_f)_{OH}}{S(N_f)_{FH}} = \frac{\alpha_{FH} \cdot \beta_{FH} \cdot K_{tg}}{\alpha_{OH} \cdot \beta_{OH} \cdot K_{tg}} \tag{8}$$

The results indicate that

$$\beta_{FH}(N_f) = \frac{\alpha_{OH} \cdot \beta_{OH} \cdot S(N_f)_{OH}}{\alpha_{FH} \cdot S(N_f)_{FH}} \tag{9}$$

Where S denotes the far field stress.

Having the values for β, the values for the θ for the different load transfer configurations can be computed using Equation 10. β_{FH} in this equation can be read from the β figures in the results section according to the maximum and mean stress. α_{OH} and α_{FH} are assumed equal. The stress concentration factor for the gross area (K_{tg}) and the stress concentration factor for the bearing stress (K_{tb}) can be found in reference 7.

$$\frac{S\left(N_f\right)_{OH}}{S\left(N_f\right)_{FH}} = \frac{\alpha_{FH} \cdot \beta_{FH}\left\{K_{tb} \cdot \theta \cdot LT \cdot \frac{w}{d} + K_{tb}\left(1 - LT\right)\right\}}{\alpha_{OH} \cdot \beta_{OH} \cdot K_{tg}} \tag{10}$$

Values of θ for the Hilok configuration are shown in the results section. Rearranging, the equation for θ yields

$$\theta = \frac{\frac{S\left(N_f\right)_{OH} \cdot \beta_{OH} \cdot K_{tg}}{S\left(N_f\right)_{FH} \cdot \beta_{FH}} - K_{tb}\left(1 - LT\right)}{K_{tg} \cdot LT \cdot \frac{w}{d}} \tag{11}$$

Finally, having β and θ, the SSF as a function of the far field stress can be calculated the following equation:

$$SSF = \alpha\beta\left(K_{tb} \times \theta \times LT \times \frac{w}{d} + K_{tg}\left(1 - LT\right)\right) \tag{12}$$

Where $LT = \Delta P / P$

Using the assumption presented in Equation 7, the SSF can be used to predict different S-N curves. For example, given the S-N data for OH (SSF = 3), the life for SSF = 2.6 can be calculated as follows. Equation 7 can be rewritten as:

$$\frac{S_{\max}(N_f)^{@\ \mathrm{SSF_{Any}}}}{S_{\max}(N_f)^{@\ \mathrm{SSF_{OH}}}} = \frac{SSF_{OH}}{\mathrm{SSF_{Any}}} \tag{13}$$

and the SSF Ratio calculated as

$$\text{SSF Ratio} = \frac{SSF_{OH}}{\mathrm{SSF_{Any}}} = \frac{3}{2.6} = 1.15 \tag{14}$$

With this SSF Ratio, the S-N curve for SSF = 2.6 can be calculated as shown in Equation 15 and Figure 3.

$$S_{\max}^{@\ SSF_{Any}} = (\text{SSF Ratio}) \cdot S_{\max}^{@\ SSF_{OH}} \tag{15}$$

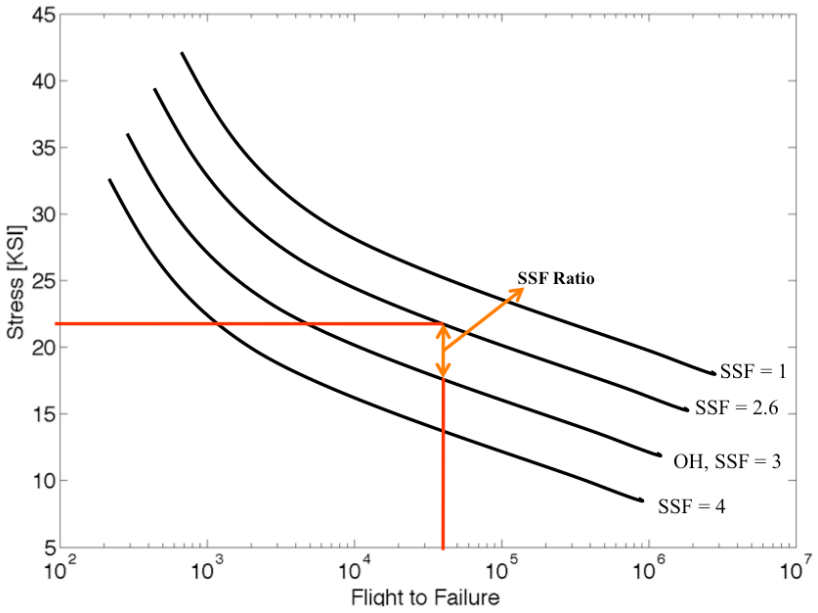

Figure 3. SN Prediction Using Open Hole Data and SSF

B. Random D Development

Using the P-S-N curves developed in the previous section, a Failure Damage Index was constructed for different usage levels and SSF levels. The flowchart presented in Figure 4 and Figure 5 shows a schematic of the steps of this methodology. The methodology was implemented in a computer code.

The methodology to generate the Failure Damage Index is briefly explained as follows:

- As shown in Figure 4, stress spectrums for two different aircraft usages (Normal and Acrobatic) and three stress levels (low, medium, and high) were generated using the guidelines contained in Federal Aviation Administration (FAA) report AFS-1208. The stress spectrum was used for the variable amplitude testing to compute the flights/cycles-to-failure. Examples of the testing results are shown in Table 2.

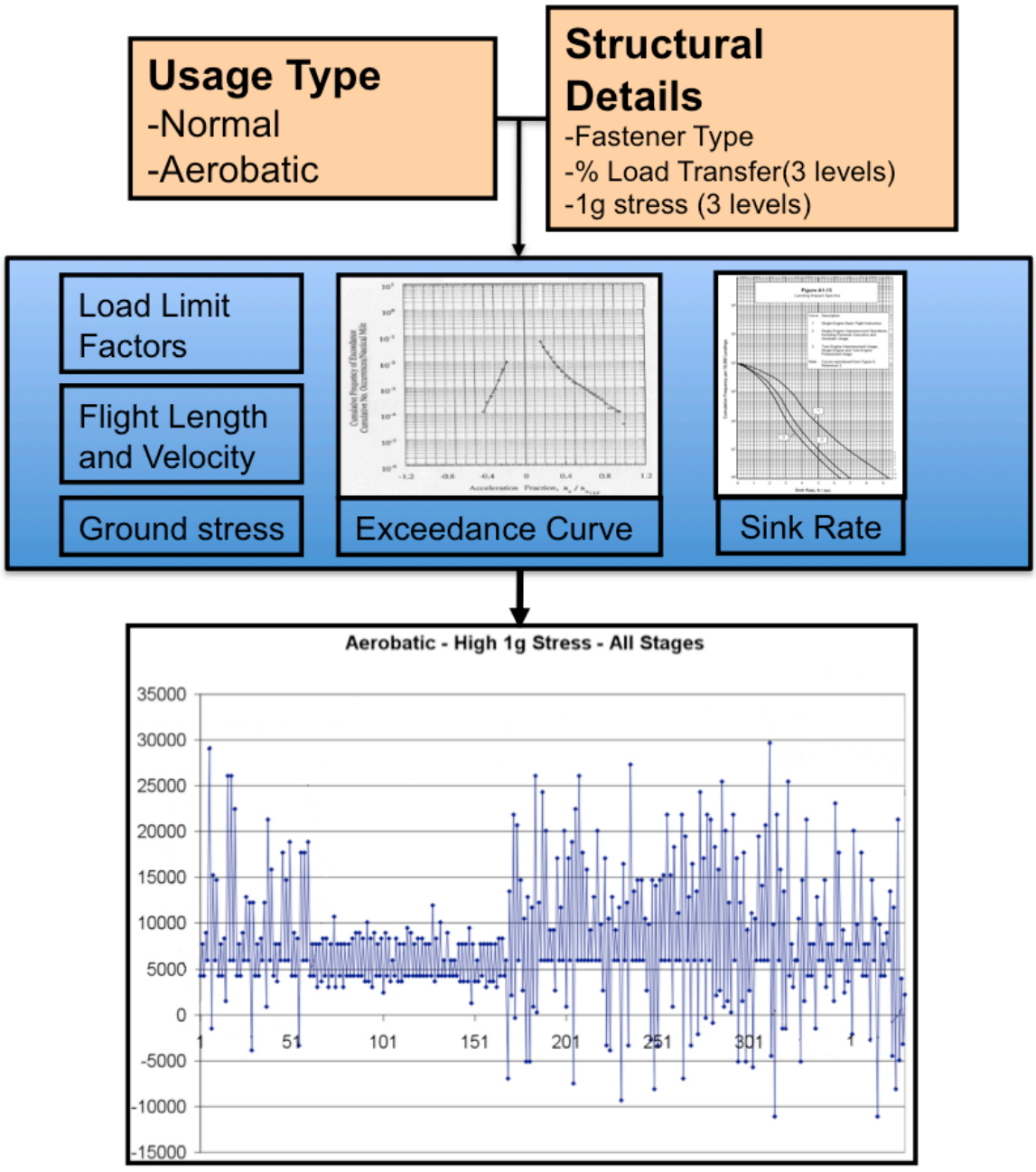

Figure 4 Random Miner's Stress Spectrum Flowchart.

- Utilizing the same spectrums used during testing and the P-S-N curves developed from constant amplitude tests, the life for each stress pair within the spectrum was calculated and stored. The spectrum was repeated until the number of simulated flights equaled the flights-to-failure from test. At the end, the damage for each of the load pairs for all the flights simulated from the spectrum results (see Table 2) were added and the failure index determined as shown in Figure 5.
- The process was repeated for the total number of variable amplitude tests, ten for normal and six for acrobatic; and then replicated inside a Monte Carlo simulation for different

realizations of S-N curves. Using these data, failure damage index probability distributions were developed.

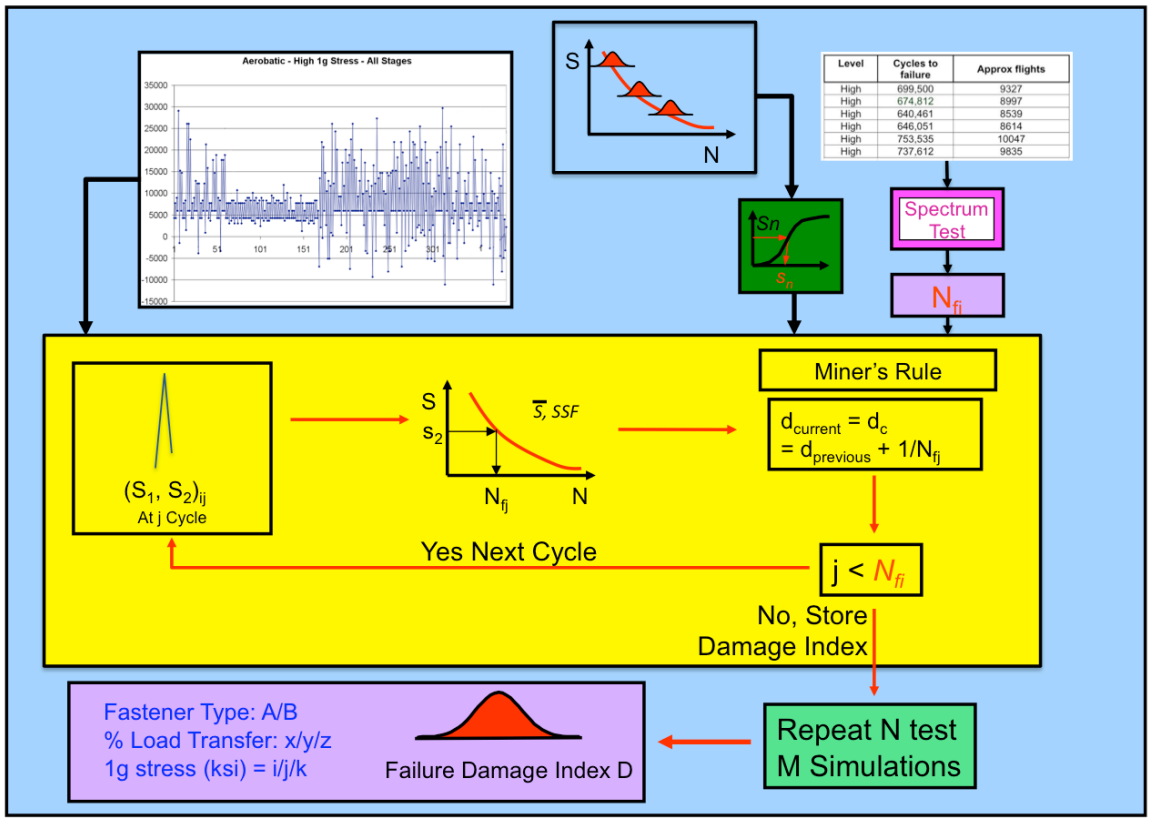

Figure 5 Random Miner's Damage Index Accumulation Flowchart.

Level	Cycles to failure	Approx flights
High	699,500	9327
High	674,812	8997
High	640,461	8539
High	646,051	8614
High	753,535	10047
High	737,612	9835
Median	2,966,231	39550
Median	3,021,865	40292
Median	2,883,978	38453
Median	2,232,472	29766
Median	3,239,215	43190
Median	3,473,815	46318
Median	2,814,230	37523
Low	9,732,139	129762
Low	12,960,957	172813
Low	11,430,769	152410
Low	10,103,299	134711
Low	12,927,999	172373
Low	10,290,617	137208

Table 2. WSU Spectrum Testing Results for Normal Usage

III. Results

Three different P-S-N curve results are shown as follows. Each figure shows the mean value, the 95 percent confidence bounds (CB), and the test data[4] (blue circles).

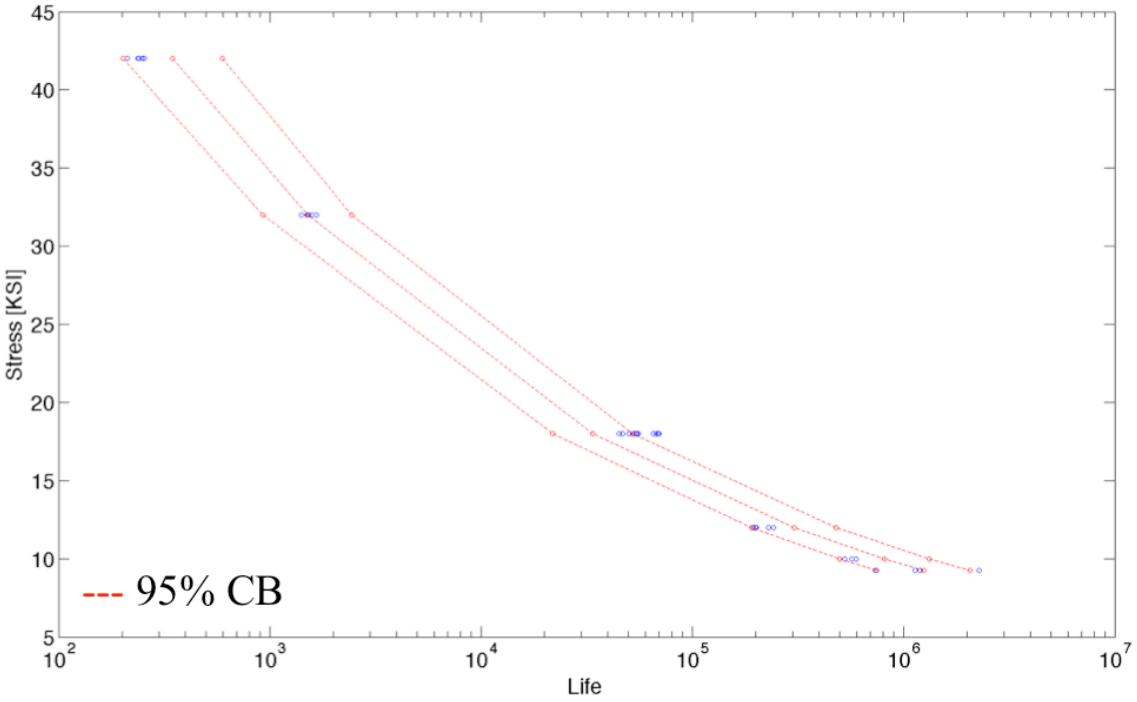

Figure 6. Open Hole 3 KSI Mean Stress

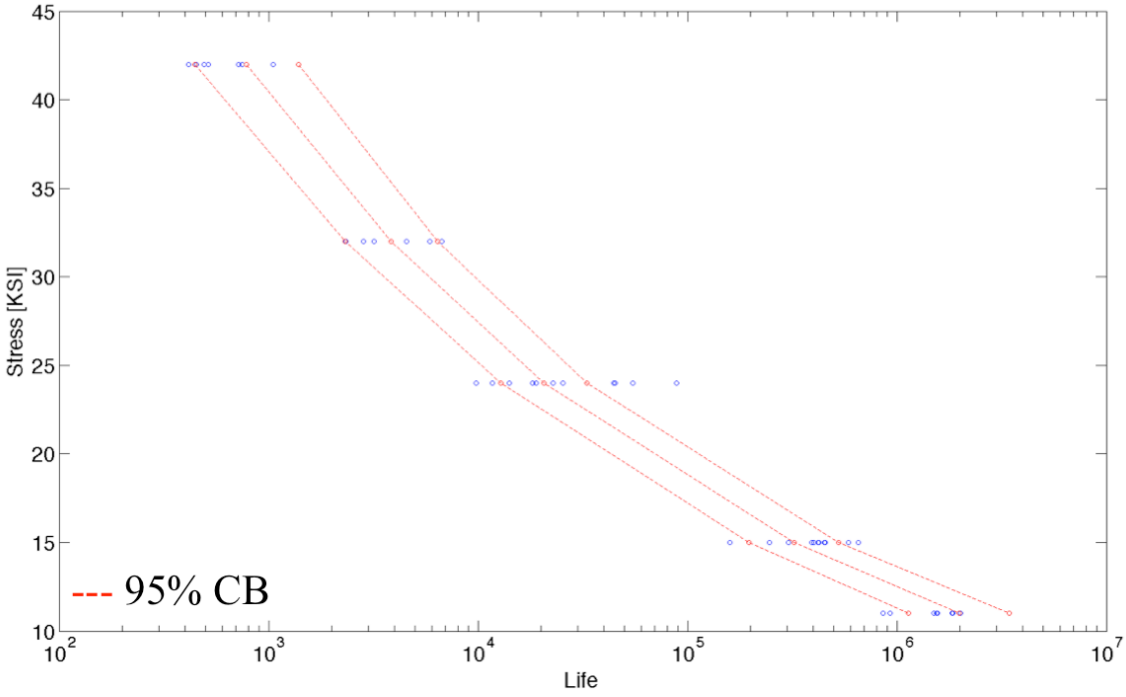

Figure 7. Hilok Fastener 6 KSI Mean Stress 50% Load Transfer

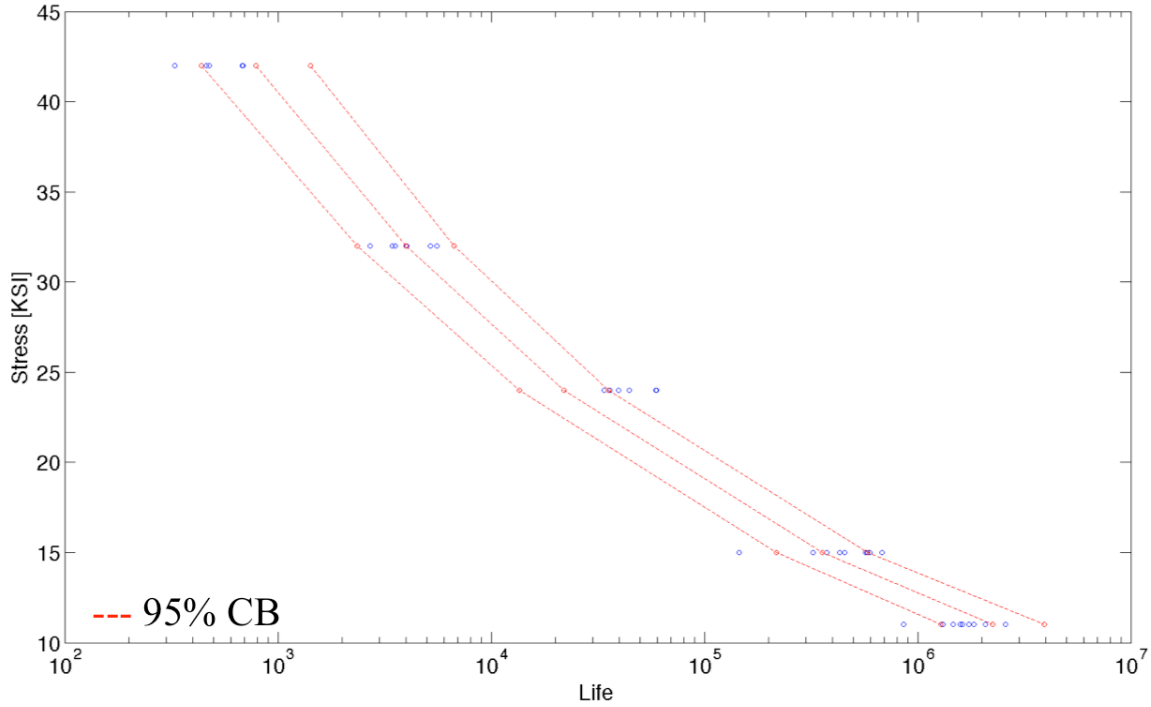

Figure 8. Hilok Fastener 6 KSI Mean Stress 30% Load Transfer

β values for the Hilok fastener are shown in Figure 9 (3 KSI mean stress) and Figure 10 (6 KSI mean Stress) as a function of the far field stress including the 95 percent confidence bounds.

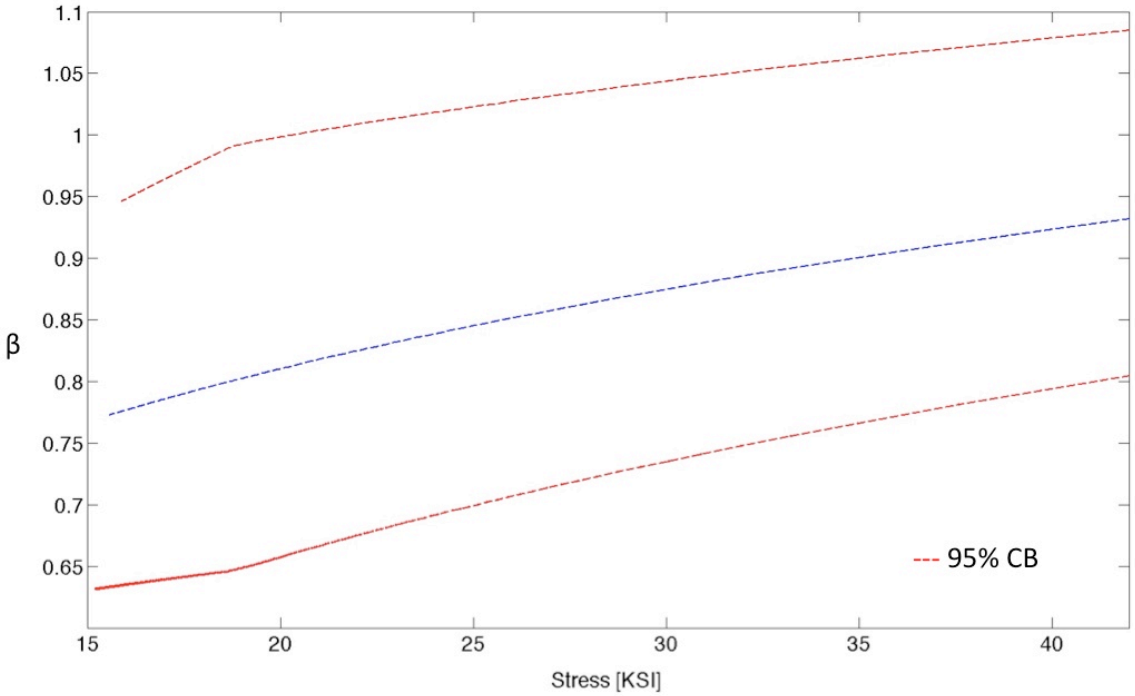

Figure 9. Beta Factor Hilok 3 KSI Mean Stress

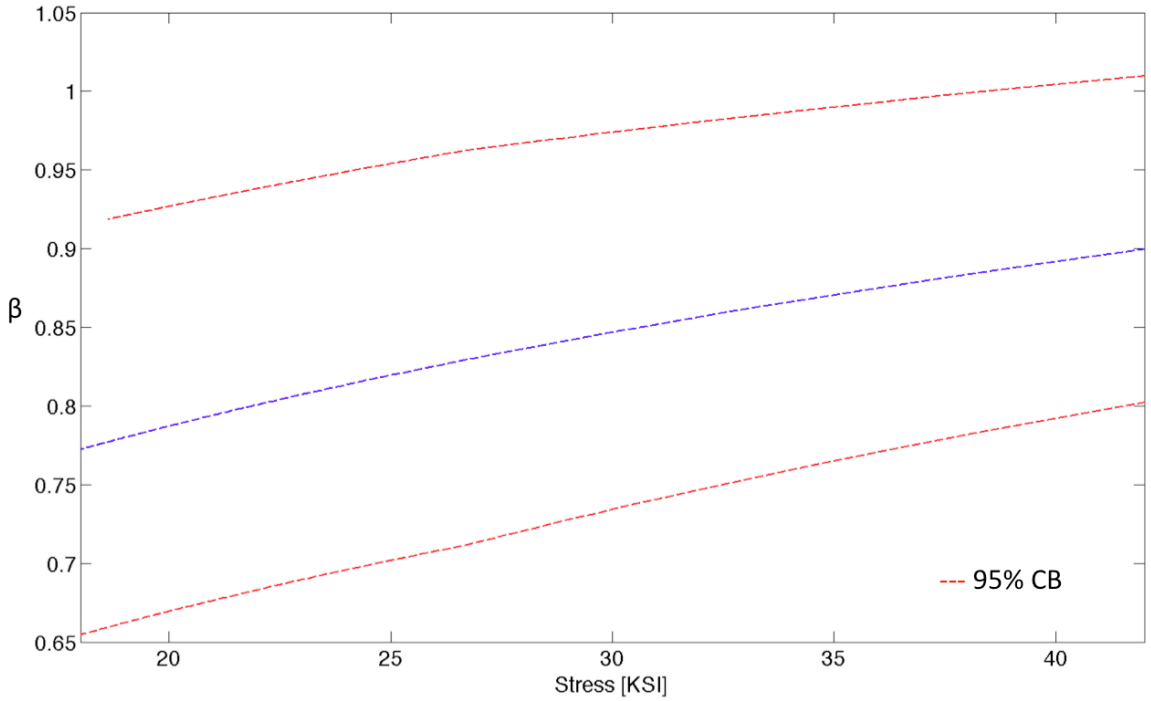

Figure 10. Beta Factor Hilok 6 KSI Mean Stress

θ factors are shown in Figure 11 (3 KSI mean stress) and Figure 12 (6 KSI mean Stress) as a function of the far field stress with its 95 percent confidence bounds.

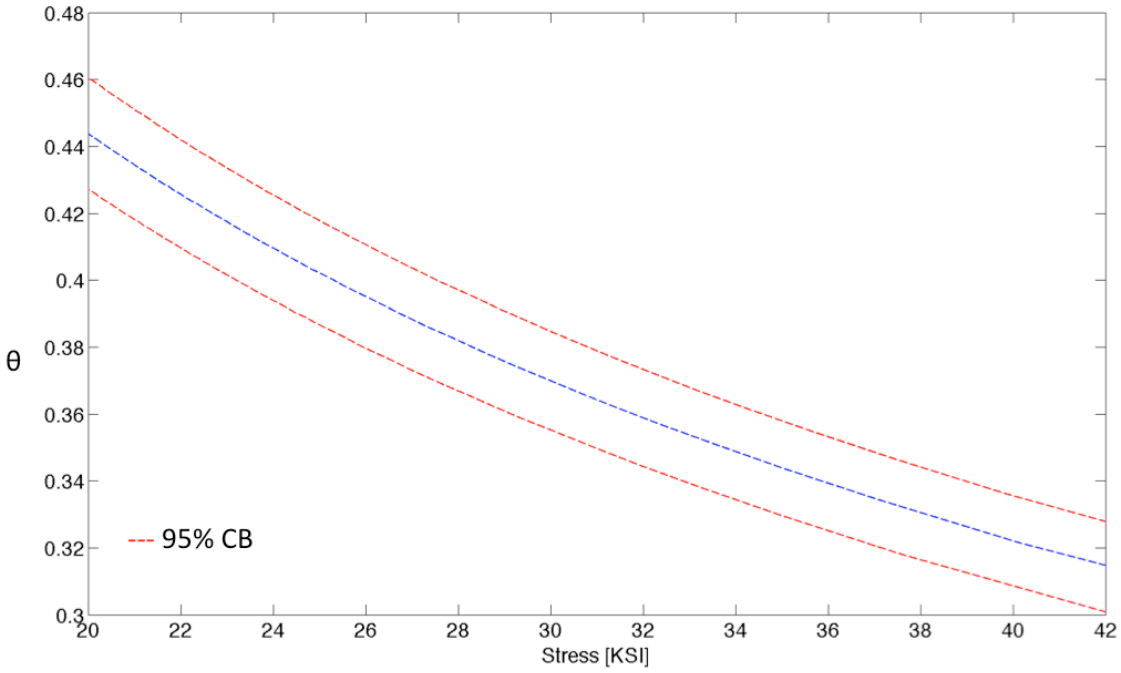

Figure 11. Theta Factor Hilok 3 KSI Mean Stress 50% Load Transfer

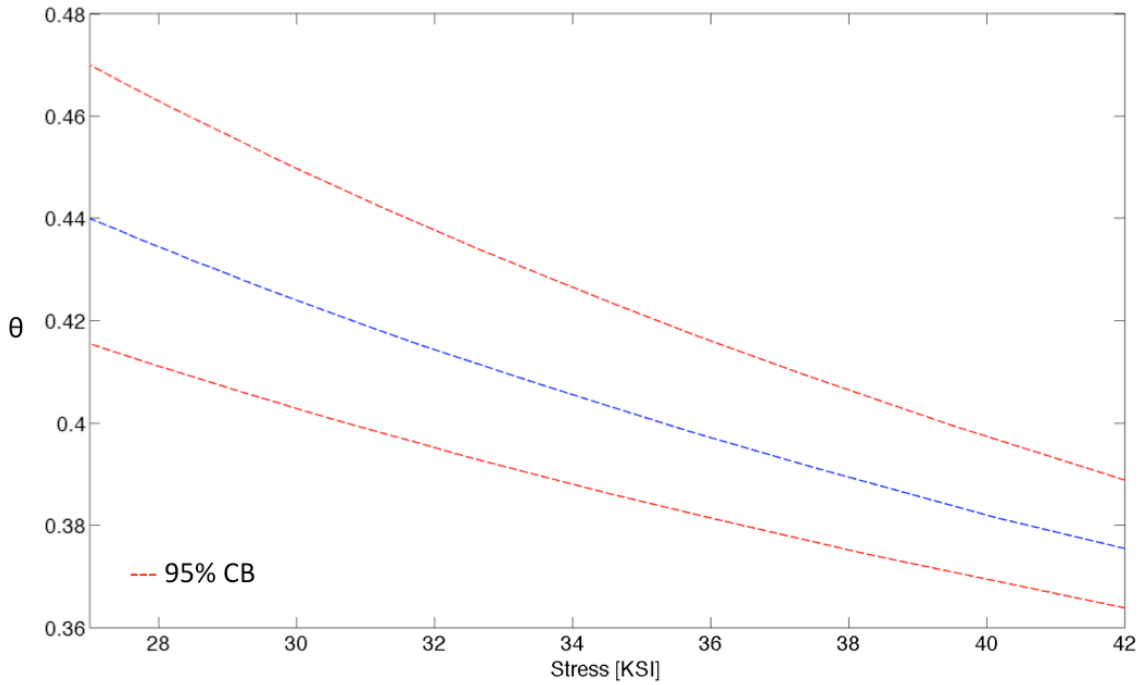

Figure 12. Theta Factor Hilok 6 KSI Mean Stress 50% Load Transfer

SSF curves as a function of the stress are shown in Figure 13 and Figure 14 with the mean value in blue and 95 percent confidence bounds in red.

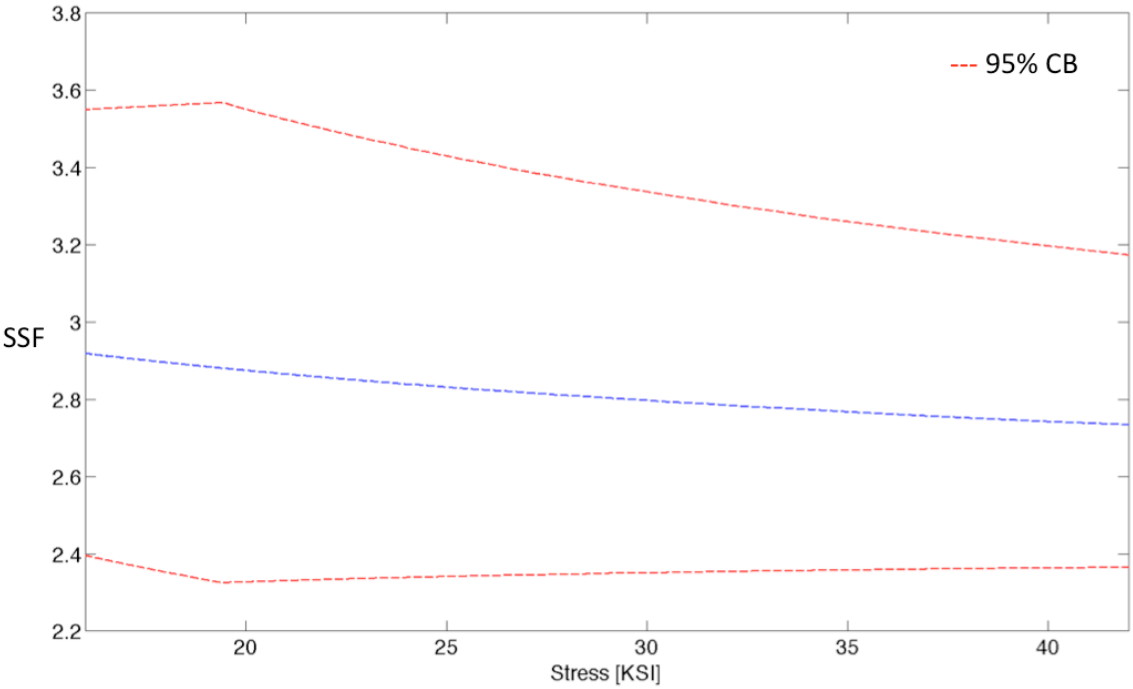

Figure 13. SSF Factor Hilok, 50% LT and 3 KSI Mean Stress

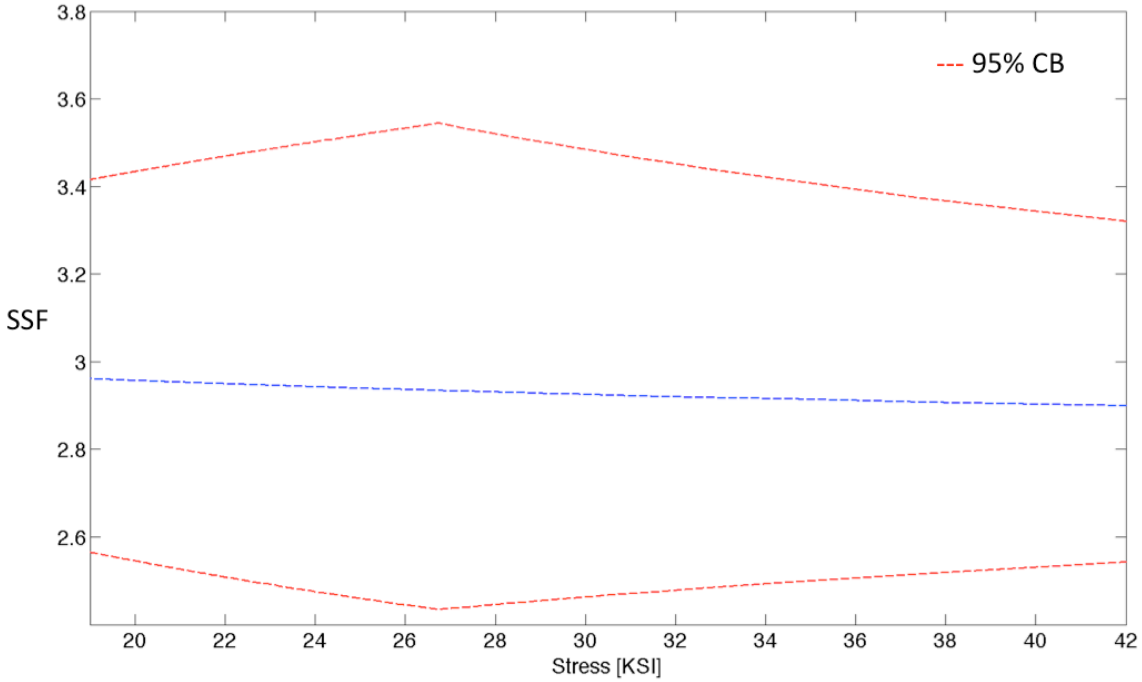

Figure 14. SSF Factor Hilok, 50% LT and 6 KSI Mean Stress

The random Failure Index Damage for two different usage spectrums at three different 1g-stress levels for four different coupons configurations was calculated and summarized in Table 3.

Spectrum	Severity	Coupon Configuration	Mean Damage Index	Coefficient of Variation
Normal	High (9 KSI)	Open Hole	0.7248	0.113
Normal	Medium (7 KSI)	Open Hole	0.8774	0.190
Normal	Low (5 KSI)	Open Hole	0.7281	0.228
Normal	High (9 KSI)	50% Load Transfer	5.7379	0.483
Normal	Medium (7 KSI)	50% Load Transfer	2.2056	0.437
Normal	Low (5 KSI)	50% Load Transfer	Coupon did not fail during testing	
Aerobatic	High (6 KSI)	Open Hole	0.8942	0.101
Aerobatic	Medium (4.5 KSI)	Open Hole	0.9151	0.131
Aerobatic	Low (3 KSI)	Open Hole	0.7495	0.135
Aerobatic	High (6 KSI)	50% Load Transfer	2.4138	0.225
Aerobatic	Medium (4.5 KSI)	50% Load Transfer	4.3957	0.468
Aerobatic	Low (3 KSI)	50% Load Transfer	Coupon did not fail during testing	

Table 3. Random Damage Index Summary Results

The Damage Index values were tested against a number of probability distributions to determine the best fit. The Weibull distribution was the best distribution for all the different cases according to Kolmogorov-Smirnov, Anderson-Darling, and Chi-Squared tests for goodness of fit, as well as from probability plots.

Probability density functions for some of the results are shown in the following figures.

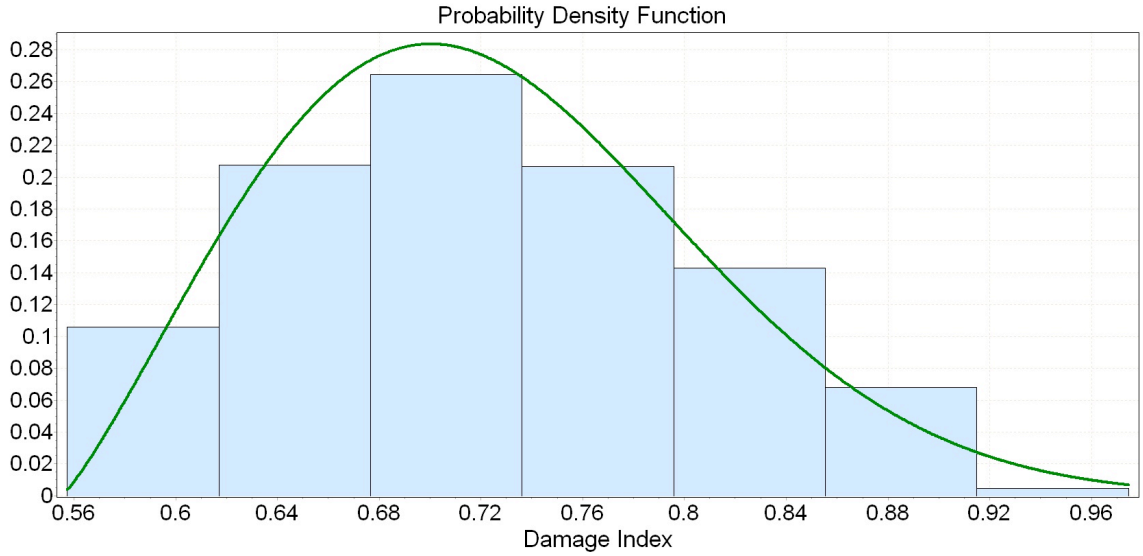

Figure 15. Probability Density Function Normal Usage, High Severity, and Open Hole

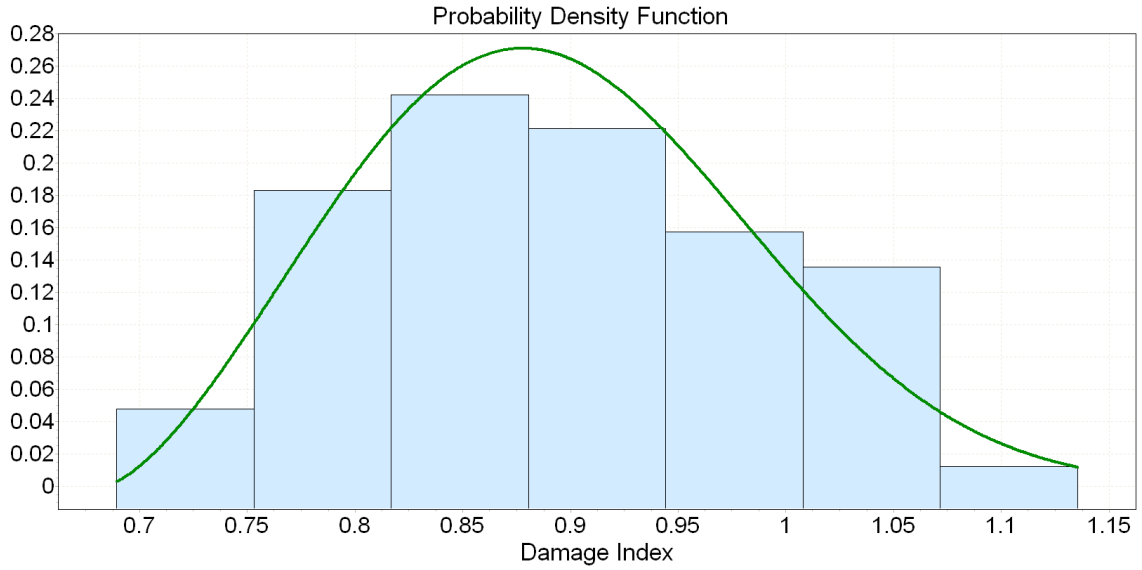

Figure 16. Probability Density Function Aerobatic Usage, High Severity, and Open Hole

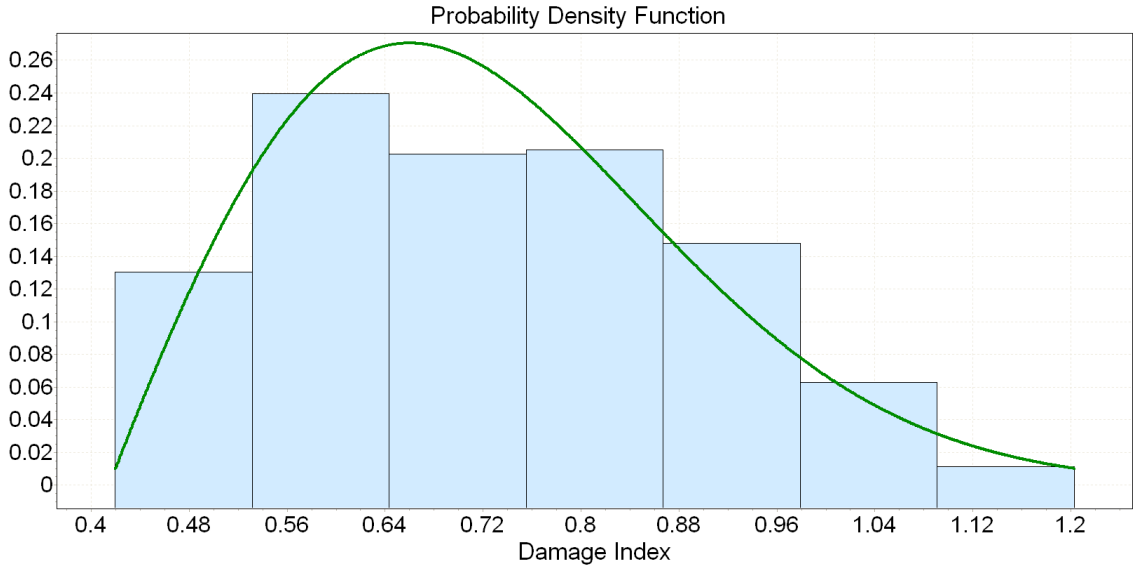

Figure 17. Probability Density Function Normal Usage, Low Severity, and Open Hole

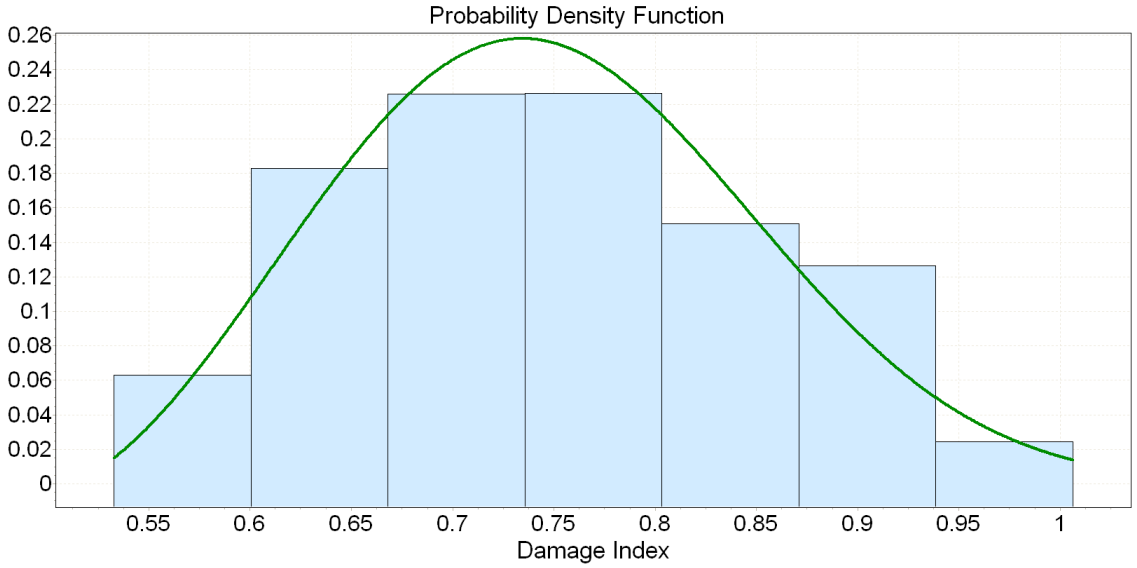

Figure 18. Probability Density Function Aerobatic Usage, Low Severity, and Open Hole

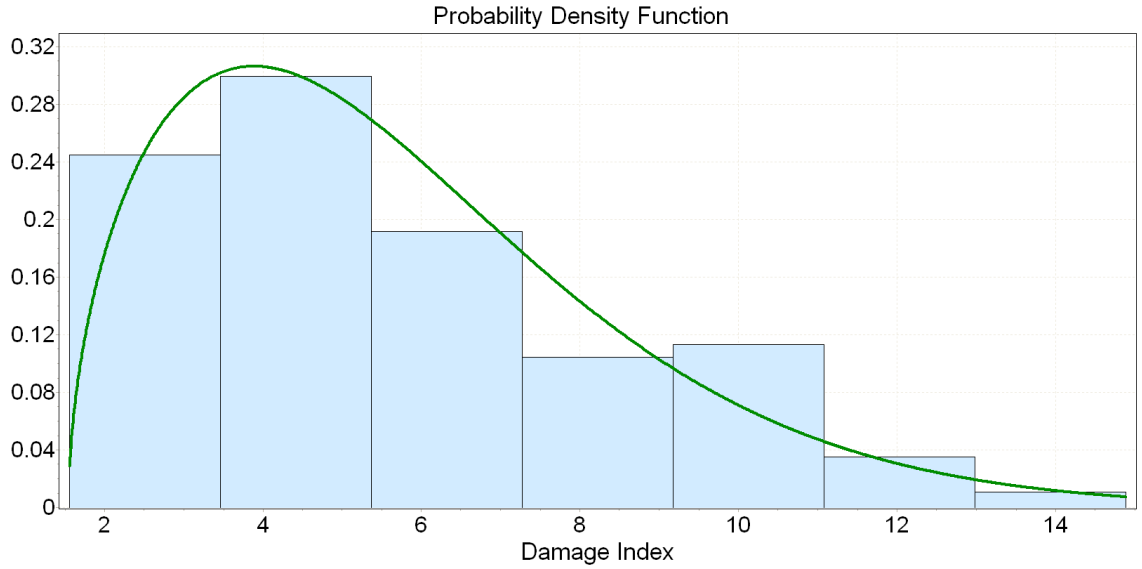

Figure 19. Probability Density Function Normal Usage, High Severity, and 50% Load Transfer

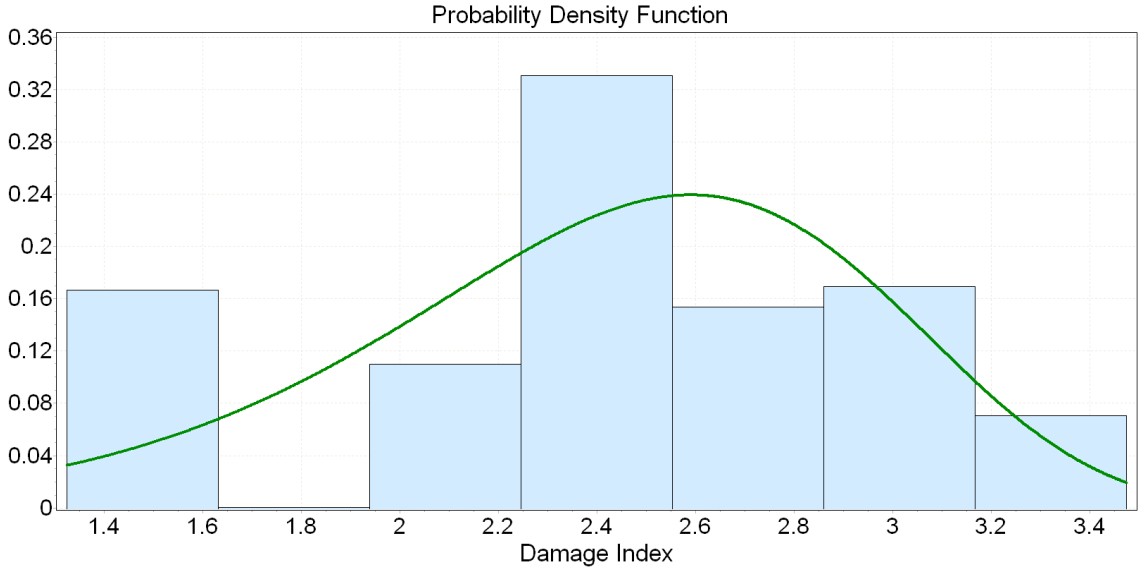

Figure 20. Probability Density Function Aerobatic Usage, High Severity, and 50% Load Transfer

IV. Conclusions

Numerous comparisons with test results show that failure occurs for a range of damage index values and the results are case and material dependent. For this reason, a probabilistic methodology and computer code were developed so that a probabilistic damage index can be calculated.

Results confirm that failure does not always occur when Miner's coefficients reaches a value equal to one. The results for *D* were best represented by a Weibull distribution with the mean values ranging from approximately 0.72 for low severity Normal usage open hole coupon to 5.73

for high severity normal usage 50% load transfer coupon, and from 0.74 for low severity Acrobatic open hole coupon to 4.39 for high severity acrobatic usage 50% load transfer.

For OH specimens with Normal usage, values ranged from 0.72 to 0.87 and for Aerobatic usage from 0.74 to 0.91. For load transfer coupons with Normal usage, the failure index ranged from 2.2. for medium severity to 5.7 with high severity. For load transfer coupons with Aerobatic usage, the failure index ranged from 2.2 for high severity to 4.4 with medium severity The higher mean damage index presented in the coupons with load transfer confirms that the bypassing load through the fastener helps to improve the life of the structure.

Probabilistic stress-life (P-S-N) curves and random damage index can be used within a probabilistic fatigue assessment of general aviation and the methodology can be extended to any structural fatigue evaluation.

V. Acknowledgments

The authors are grateful to the Federal Aviation Administration (FAA) for grant 07-G-011 which supports this research project.

VI. References

[1] Miner M. A., "Cumulative Damage in Fatigue." Journal of Applied Mechanics, 1945, pp. A159-A164.
[2] Schijve J., "Fatigue of Structures and Materials." Norwell, MA: Klumer Academics Publishers; 2001.
[3] Manson S. S., and Haldford G. R., "Practical Implementation of the Double Linear Damage Rule and Damage Curve Approach for Treating Cumulative Fatigue Damage." International Journal of Fracture, 1981, pp. 169-192.
[4] Raju, K.S., Smith, K.S., Caido, F., Gomez, C., Shiao, M., "Fatigue Behavior of Fastener Joints." SAE International Journal of Aerospace, Vol. 1 No.1, 2009, pp 675-684.
[5] Jarfall, L., "Optimum design of joints: the stress severity factor concept, Aircraft Fatigue, Design, Operational and Economic Aspects." Pergamon, Australia, J.Y. Mann and I.S. Milligan Eds., 1972, pp. 337-380.
[6] ASTM E739-91 (Reapproved1998), Statistical Analysis of Linear or Linearized Stress-Life (S-N) and Strain-Life (e-N) Fatigue Data (1998).
[7] Niu, C.Y., "Airframe Structural Design." Granada Hills, CA: ADASO/ADASTRA Engineering Center. 2006.
[8] FAA Report AFS120-73-2, "Fatigue Evaluation of Wing and Associated Structure on small Airplanes." 1973.